RAPID COMMUNICATIONS

PHYSICAL REVIEW B VOLUME 59, NUMBER 12 15 MARCH 1999-II

Single-atom motion during a lateral STM manipulation

Xavier Bouju*
Laboratoire de Physique Moléculaire, UMR CNRS 6624, Université de Franche-Comté, La Bouloie, F-25030 Besançon Cedex, France

Christian Joachim and Christian Girard
Centre d'Élaboration des Matériaux et d'Études Structurales, UPR CNRS 8011, 29, rue Jeanne-Marvig, Boîte Postale 4347,
F-31055 Toulouse Cedex 4, France

(Received 7 January 1999)

We report on the numerical implementation of a *virtual* scanning tunneling microscope which calculates imaging and manipulation modes and reproduces a *feedback loop signal* (FLS). Calculating the FLS during a manipulation serves as a direct diagnostic of the mechanics of the adsorbate under the tip apex because pulling, sliding, or pushing modes have their own FLS signatures independently of the manipulated species. As an example, the different FLS are provided for the case of a Xe atom manipulated in the constant current mode. [S0163-1829(99)51512-9]

The scanning tunneling microscope (STM) has the ability to manipulate individual atoms as first demonstrated by Eigler and Schweizer.[1] Now, atomic scale devices are assembled atom per atom (molecule per molecule) to study electronic[2] and mechanical[3] properties at the nanometer scale. These very recent developments are supported by a renewed interest in *surface science phenomena*. They have generated a large body of experimental demonstrations of both atomic and molecular manipulations[1–10] and are accompanied by few theoretical studies.[11,12]

All these manipulations require an extremely fine control of the local interactions between the STM probe tip, the adsorbate, and the surface. Moreover, they are generally performed in a *constant current mode* obtained by introducing a feedback loop between the tunnel current passing through the adsorbate and the voltage applied to the STM piezotranslator. This operating mode prevents the imaging of the adsorbate during the manipulation sequence, and the final location of the adsorbate on the surface must be checked back in the imaging mode. Recently, it has been proposed[9,12] that the STM *feedback loop signal* $\Delta Z(X)$ recorded during a manipulation is a *diagnostic* of the mechanics occurring in the junction during the lateral motion of the tip along the X direction. For a variety of atoms and diatomic molecules, regular signals $\Delta Z(X)$ have been observed with different saw-tooth shapes.[9] For polyatomic molecules, despite their large number of internal degrees of freedom, a careful analysis of $\Delta Z(X)$ could also provide important information on the molecular conformation changes during the motion.[14]

We show, in this paper, that the analysis of the $\Delta Z(X)$ signals requires a *virtual* STM able, in a complete calculation, to integrate the physical phenomena involved in a manipulation: (i) the electronic structure of the junction, (ii) the molecular dynamical behavior, (iii) the tunnel current intensity, and finally (iv) the STM feedback loop.

The paper is organized as follows. We first detail the *three* basic equations that govern our *virtual* STM. This framework is then applied to the study of the drastic transformation of $\Delta Z(X)$ signal when passing from imaging to manipulation modes. Finally, it is shown that intrinsic instabilities in the junction prevent a pure *sliding* mode in which the adsorbate would always be trapped under the tip apex. Although the *virtual* STM reported in this paper applies well to many adsorbate-surface systems, it is presented here for a single Xe atom adsorbed on a Cu(110) surface.

The tunneling current intensity in an STM junction can be fitted by the exponential law:

$$I(\mathbf{R}(\tau))=I_0(V_b,\mathbf{r}_a,\mathbf{R}(\tau))\exp(-1.02\Phi^{1/2}Z(\tau)), \qquad (1)$$

where V_b represents the STM bias voltage, $\mathbf{r}_a=(x_a,y_a,z_a)$ the adsorbate position vector relative to the surface referential, $\mathbf{R}=(X,Y,Z)$ the tip-apex position vector, and Φ a local effective barrier height. At large Z, $\Phi\simeq 4-5$ eV for metal,[15] while at small Z, Φ is significantly modified by either the mechanical deformations or the electronic interactions of the adsorbate with the tip apex.[16] The prefactor I_0 depends on the detailed electronic structure of the tip apex, the adsorbate, and the surface, and τ represents the scanning time of the probe tip.

The elastic scattering quantum chemistry (ESQC) technique described in previous works[17] is used to describe this structure and to calculate Eq. (1). This technique, based on a multichannel scattering approach of $I(\mathbf{R})$, allows the full valence orbital structure of the junction as well as the band structure of the surface to be introduced. The parameters that enter this description can be standard, as, for example, the extended hückel molecular orbital method (EHMO), or extracted from *ab initio* or density functional theory calculations.[18] The effective Hamiltonian method is then used to couple the aperiodic part of the junction (formed by the adsorbate and the tip-apex subsystem) with the bulk interface (composed of the sample and the tip-body environment). In the case of a single Xe atom, we choose the metallic surroundings already described in recent van der Waals trap calculations.[12] This geometry consists of a cluster of 14 copper atoms [110] oriented and adsorbed on the (110) surface of the tip body. The other part of the junction is a Cu(110) surface supported by its bulk.

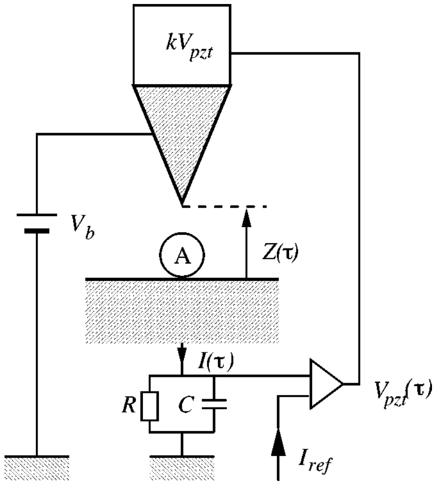

FIG. 1. Schematic electric circuit diagram of a standard STM junction. The circle schematizes the adsorbate, $I(\tau)$ is the tunnel current, and V_{pzt} represents the voltage applied to the piezotranslator. The feedback loop is filtered by the RC circuit (corresponding to a RC time constant of 0.1 s for Xe).

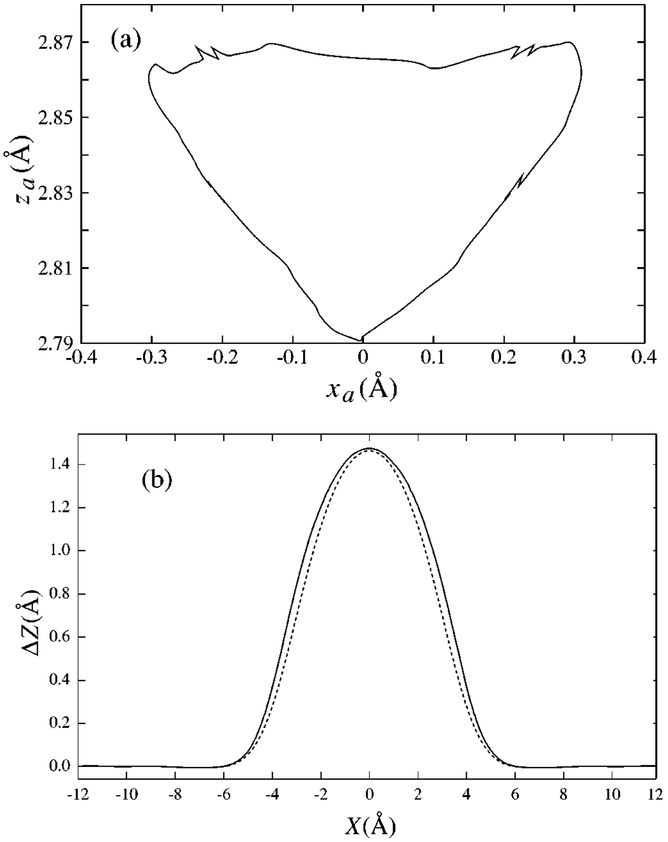

FIG. 2. (a) Lateral motion of the Xe atom during a complete imaging scan at $I_{ref}=1$ nA and $V_b=10$ mV. (b) Variation of the apparent shape of the atom for a dynamical calculation (solid curve) and for a configuration where the adsorbate is kept frozen in its equilibrium site (dashed curve).

Inside this environment, the behavior of the Xe atom can be treated by the classical mechanics using a molecular dynamics (MD) scheme:

$$m_a\ddot{\mathbf{r}}_a(t) = -\nabla U_a(\mathbf{r}_a,\mathbf{R},t) - \eta_a m_a \dot{\mathbf{r}}_a(t), \qquad (2)$$

where m_a represents the mass of the adsorbate. The parameter η_a (1.4×10^{10} s^{-1} in our Xe example) accounts for the weak energy damping introduced by the surface phonons.[19] At this point, it is important to stress that the *adsorbate* time t differs from the scanning time τ of the tip motion ($t \ll \tau$). Actually, the atomic time occurring in Eq. (2) is sampled from the atomic relaxation time η_a^{-1} so that the adsorbate can be stabilized in the junction before each new scanning step.

The potential energy U_a can be calculated from different techniques, including (i) standard molecular mechanical and dynamical approaches with pairwise interactions,[13,11,14] (ii) semi-empirical approximations (like the atom superposition and delocalization technique) (Ref. 20) compatible with the EHMO description or more sophisticated calculations. In the case of a single Xe atom localized in the above-mentioned metallic junction, a precise many-body self-consistent approach[12] was used to recreate the so-called van der Waals trap generated under the tip apex.

In an experimental STM setup, a low-pass filter in the feedback loop efficiently avoids the mechanical instabilities of the junction and the loop oscillations. The feedback loop of our virtual STM (Fig. 1) operates also with such a low-pass filter. Assuming a linear relation $Z=kV_{pzt}$, with the bias voltage V_{pzt} applied to the piezotranslator, the first-order differential equation relating $I(\tau)$ and $Z(\tau)$ is given by

$$I(\tau)=\frac{C}{k}\frac{dZ(\tau)}{d\tau}+\frac{Z(\tau)}{kR}+I_{ref}, \qquad (3)$$

where RC is the time constant of the low-pass filter and I_{ref} the reference current. A numerical STM should be based on the numerical solving of these three coupled time-dependent equations [Eqs. (1)–(3)] simultaneously. Nevertheless, for a constant I_{ref} mode of operation and to speed up the numerical procedure, it is more efficient to solve iteratively Eqs. (1) and (2). Beginning with a junction configuration $\{\mathbf{r}_a^i,\mathbf{R}^i\}$, the virtual STM first determines the configuration $\{\mathbf{r}_a^i,\mathbf{R}^j\}$ that corresponds to I_{ref}, thanks to Eq. (1). This junction status is then used as initial conditions in Eq. (2). After relaxation of the Xe atom, Eq. (2) gives back a new configuration $\{\mathbf{r}_a^j,\mathbf{R}^j\}$ allowing the next numerical step to be performed. The relaxed junction configuration j is not identical to the I_{ref} configuration i required by the feedback loop. This generates instabilities in the virtual STM feedback loop due to this external I_{ref} constraint applied to the adsorbate-tip system. According to Eq. (3), the junction configuration is numerically stabilized by both a low-pass filtering and a sequence of current and molecular dynamics computations. For $I_{ref}=1$ nA and a bias voltage $V_b=10$ mV, an apparent $\Delta Z \simeq 1.5$ Å height of the atom is found in excellent agreement with the experimental data by Eigler and Schweizer.[1] We observed that, even in the imaging mode—in which the tip interacts very weakly with the Xe atom in its adsorption site—the competition between (i) the *adsorbate position* imposed by the reference current I_{ref} and (ii) the *adsorbate position* controlled by the mechanics, induces a residual motion of the Xe atom upon imaging. In particular, it produces a significant apparent width enlargement [Fig. 2(a)]. A broadening of about 0.8 Å in the Xe atom image is deduced

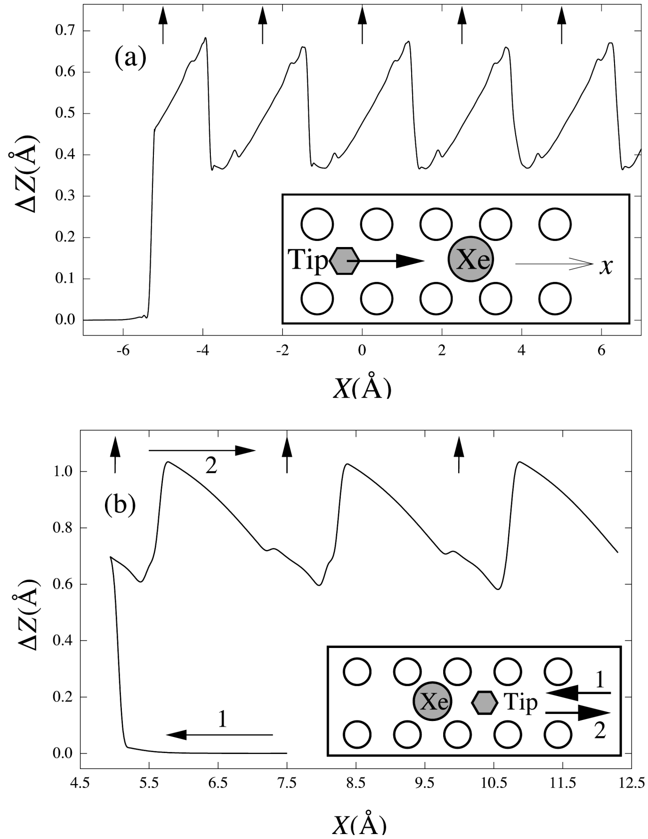

FIG. 3. Two feedback loop STM signals illustrating the (a) pushing with $I_{ref}=6.5$ nA and (b) pulling with $I_{ref}=4$ nA manipulation modes. The insets give a snapshot of the tip-adsorbate configuration and the small vertical arrows point to the hollow sites along the atomic row of the (110) surface.

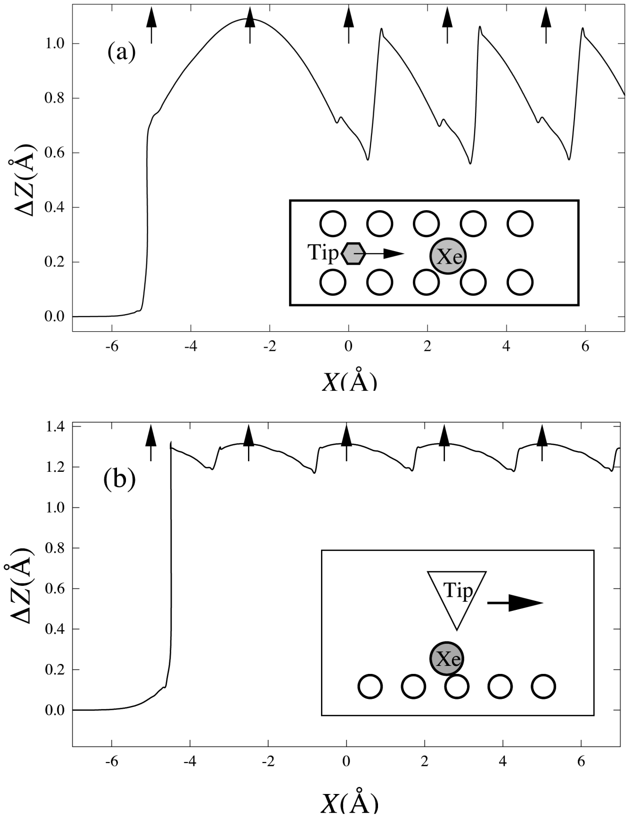

FIG. 4. Simulation of two other saw-tooth patterns with an initial configuration defined by $\{x_a=0, X=-7\ \text{Å}\}$. (a) Pulling mode with a reference current fixed at 4 nA. (b) Sliding-pulling mode (obtained with $I_{ref}=1.9$ nA) in which the atomic motion remains very localized under the tip.

from the comparison between dynamical and static calculations [Fig. 2(b)].

Our virtual STM predicts only three different classes of $\Delta Z(X)$: a periodic saw-tooth signal where $\Delta Z(X)$ is discontinuous at the end of each period, a quasisinusoidal signal, and a periodic saw-tooth signal where the discontinuity arises at the beginning of each period. The chemical nature of the adsorbate will only determine the initial approach of the tip apex and impose I_{ref} to reach a particular periodic $\Delta Z(X)$ signal. For example, with $I_{ref}=6.5$ nA and when the tip is approached as indicated in the inset of Fig. 3(a), the tip begins a series of regular saw-tooth Z motions with an amplitude $\Delta h=0.29$ Å [Fig. 3(a)]. The period of these oscillations is commensurate with the surface atomic spacing along the $[1\bar{1}0]$ manipulation direction. This $\Delta Z(X)$ signal is characteristic of a *pure pushing* mode where the adsorbate is first repelled and then recaptured by the tip apex. The recurrent sharp decrease of $\Delta Z(X)$ is due to this repulsion effect since the tunnel junction resistance increases when the Xe atom is away from the tip apex. In this pushing mode, the Xe atom interacts laterally with the tip apex via an effective quadratic term with respect to the distance that accounts for the potential energy. The Δh amplitude then yields a direct measurement of the stiffness of this springlike effect. A small Δh indicates a strong back force of the adsorbate towards the tip apex.

The second example [Fig. 3(b)] presents a signature specific to a *pure pulling* mode. In order to perform a lateral pulling of the Xe atom, we have found that the tip must be first approached progressively and then retracted in front of the atom. For $I_{ref}=4.0$ nA and at a threshold tip-adsorbate lateral distance of ~5.0 Å, the Xe atom is captured by the tip apex. In this new manipulation mode, the tip always precedes the atom. There is a significant increase of Δh(0.45 Å) with a concommitant inversion of the saw-tooth signal with respect to the one of the pushing mode. The effective lateral spring constant of the interaction is now softened and the tip apex can manipulate the Xe atom at larger distances than in the pushing mode.

A full exploration of the stability map associated with these various situations, indicates that in the presence of a single Xe atom, the junction resistance R_{junc} varies between 10 and 1.6 MΩ when we are continuously passing from the imaging to the pushing mode. Around a resistance range close to 2.5 MΩ, we have found a rich variety of pulling modes at the transition between the imaging and the pushing modes. For example, when the tip apex starts in a pushing mode configuration, it can image the atom, pass over it and then reach a pure pulling mode [Fig. 4(a)]. At the threshold of the imaging mode, we have tried to stabilize a pure sliding mode of manipulation[4] where the Xe atom would remain exactly trapped under the tip apex during the manipulation, resulting in pure sinusoidal $\Delta Z(X)$. For $R_{junc}=5.26$ MΩ, we have found a very interesting *pulling-sliding* mode as a mix between a pulling mode and what would be an ideal sliding mode. A quasisinusoidal shape of the $\Delta Z(X)$ signal is observed and Δh reduces drastically to reach a value lower than 0.1 Å [Fig. 4(b)]. Nevertheless, whatever the initial tip approach may be (back, as in a pushing mode, top,[4] or in front, as in a pulling mode), a pure sliding manipulation seems not possible. When the atom is trapped just at the tip apex, its mechanical equilibrium near a bridge site of the surface is always instable because of the constraint imposed by I_{ref}. This explains why even a soft top approach is not sufficient to trap the Xe atom exactly at the tip apex during a manipulation.

Similar $\Delta Z(X)$ signals have been obtained experimentally by Bartels and coworkers[9] with two different metal atoms. In particular, a pulling mode is clearly identifiable on the experimental $\Delta Z(X)$ for both a single Cu and a single Pb atom adsorbed on the Cu(211) surface [cf. Figs. 2(a) and 2(b) in Ref. 9]. These data also confirm that the preparation of a successful pulling mode depends on the chemical nature of the adsorbate. The information on this transitory regime is encoded in the first period of the $\Delta Z(X)$ signal. While for a Xe atom, the preparation of a pulling mode requires a quasicomplete scan over it with the tip initially positioned at the left of the Xe [Fig. 4(a)], only a partial lateral scan is necessary for a Pb atom [cf. Fig. 2(b) in Ref. 9]. A sliding motion with a typical sinuslike $\Delta Z(X)$ signature has also been recorded with a Pb atom adsorbed on a stepped vicinal surface [cf. Fig. 2(c) in Ref. 9]. As mentioned above, it is not possible to achieve a close trapping of the Xe atom on a perfectly plane surface just under the tip in a sliding mode. For a Pb atom, further detailed studies must confirm whether or not the observed sinusoid corresponds to a pure sliding mode where the atom is trapped under the tip-apex end atom during the tip motion. Note that pushing motion remains to be observed for Pd and Cu atoms. For each manipulation mode, the STM junction resistance is larger for Xe than for Cu or Pd because of the small density of states introduced at the Fermi level by Xe compared to Cu or Pb.

In conclusion, our *virtual* STM reproduces successfully the *macroscopic* feedback loop signal output of an STM and relates it to the mechanical events occurring at the *atomic* scale inside the junction. As a first application, we have classified the different manipulation modes of a single Xe atom, showing in particular that a pure sliding mode cannot be stabilized. The three different classes identified by our virtual STM are general and independent of the adsorbate under consideration. Although, for each class, both threshold and resistance ranges depend clearly on the potential energy U_a experienced by the adsorbate, the global shape of the feedback loop signatures remains independent of the nature of this potential. These signatures indicate three stable dynamic behaviors for a tip-apex–adsorbate–surface system under the influence of a macroscopic feedback control. In consequence, these new tools can also be used for describing manipulation of a large variety of adsorbates provided the potential U_a is adapted for each new system.

---

*Electronic address: xavier.bouju@univ-fcomte.fr

[1] D. M. Eigler and E. K. Schweizer, Nature (London) **344**, 524 (1990).

[2] M. F. Crommie, C. P. Lutz, and D. M. Eigler, Science **262**, 149 (1993).

[3] J. K. Gimzewski, C. Joachim, R. R. Schlitter, V. Langlais, H. Tang, and I. Johannsen, Science **281**, 531 (1998).

[4] J. A. Stroscio and D. M. Eigler, Science **254**, 1319 (1991).

[5] G. Meyer, S. Zöphel, and K.-H. Rieder, Phys. Rev. Lett. **77**, 2113 (1996).

[6] T. A. Jung, R. R. Schlittler, J. K. Gimzewski, H. Tang, and C. Joachim, Science **271**, 181 (1996).

[7] P. H. Beton, A. W. Dunn, and P. Moriarty, Surf. Sci. **361/362**, 878 (1996).

[8] J. Li, R. Berndt, and W.-D. Schneider, Phys. Rev. Lett. **76**, 1888 (1996).

[9] L. Bartels, G. Meyer, and K.-H. Rieder, Phys. Rev. Lett. **79**, 697 (1997).

[10] G. Dujardin, A. Mayne, O. Robert, F. Rose, C. Joachim, and H. Tang, Phys. Rev. Lett. **80**, 3085 (1998).

[11] A. Buldum and S. Ciraci, Phys. Rev. B **54**, 2175 (1996).

[12] X. Bouju, Ch. Girard, H. Tang, C. Joachim, and L. Pizzagalli, Phys. Rev. B **55**, 16 498 (1997).

[13] X. Bouju, C. Joachim, Ch. Girard, and Ph. Sautet, Phys. Rev. B **47**, 7454 (1993).

[14] H. Tang, M. T. Cuberes, C. Joachim, and J. K. Gimzewski, Surf. Sci. **386**, 115 (1997).

[15] G. Binnig and H. Rohrer, IBM J. Res. Dev. **30**, 355 (1986).

[16] C. Joachim, J. K. Gimzewski, R. R. Schlittler, and C. Chavy, Phys. Rev. Lett. **74**, 2102 (1995).

[17] Ph. Sautet and C. Joachim, Chem. Phys. Lett. **185**, 23 (1991).

[18] Ph. Sautet, Chem. Rev. **97**, 1097 (1997).

[19] B. N. J. Persson, Surf. Sci. **269/270**, 103 (1992).

[20] L. Pizzagalli, J.-C. Okon, and C. Joachim, Surf. Sci. Lett. **384**, L852 (1997).